

Structural Features and Properties of the Vitreous Part of the System $50P_2O_5-25CaO-(25-x)Na_2O-xCoO$ (with $0 \leq x \leq 25$; mol%)

Brahim Bachachir¹, Yassine Er-Rouissi¹, Radouane Makhoulouk¹, Achraf Harrati², Abdeslam El Bouari², Said Aqdim^{1,3*}

¹Faculty of Sciences Ain Chock, Laboratory of Materials Engineering for Environment and Valorization, Hassan II University, Casablanca, Morocco

²Faculty of Sciences Ben-M'sik, Laboratory Physical-Chemistry of Applied Materials, Hassan II University, Casablanca, Morocco

³Department of Chemistry, Faculty of Science, Mineral Chemistry Laboratory, Hassan II University Ain Chock, Casablanca, Morocco
Email: *said_aq@yahoo.fr

How to cite this paper: Bachachir, B., Er-Rouissi, Y., Makhoulouk, R., Harrati, A., El Bouari, A. and Aqdim, S. (2021) Structural Features and Properties of the Vitreous Part of the System $50P_2O_5-25CaO-(25-x)Na_2O-xCoO$ (with $0 \leq x \leq 25$; mol%). *Advances in Materials Physics and Chemistry*, 11, 254-266.
<https://doi.org/10.4236/ampc.2021.1112021>

Received: October 13, 2021

Accepted: December 26, 2021

Published: December 29, 2021*

Copyright © 2021 by author(s) and Scientific Research Publishing Inc. This work is licensed under the Creative Commons Attribution-NonCommercial International License (CC BY-NC 4.0).
<http://creativecommons.org/licenses/by-nc/4.0/>



Open Access

Abstract

The glass series $50P_2O_5-25CaO-(25-x)Na_2O-xCoO$ (with $0 \leq x \leq 25$; mol%), has been prepared by direct melting at $1080^\circ C \pm 20^\circ C$. The introduction of cobalt in calcium phosphate glasses is used to compare its effect with calcium in inhibition corrosion. The dissolution rate has been investigated. It indicated an improvement of chemical durability when the cobalt oxide increases in the network glass at the expense of Na_2O content. Both, IR spectroscopy and X-ray diffraction have confirmed the structure changes when the CoO content increases in the glass. This change results in the disappearance of isolated orthophosphate groups followed of a polymerizing of the structure from isolated orthophosphate towards pyrophosphate chains (Q^1) by promoting the formation of oligophosphates (mixed Q^1-Q^2) rich in pyrophosphates. Analysis of the density values, showed an increase of density with the increase CoO content. The covalent radius values of oxygen $r_{cal}(O^{2-})$ indicate a significant decrease and therefore a relatively high reinforcement of the metal-oxygen-phosphorus (Co-O-P) bonds. SEM micrograph confirms the evolution of the glass structural morphology. The sample having a maximum CoO content confirms a homogeneous glass phase with quite crystalline particles. This property is prerequisite for many interesting industrial applications.

Keywords

Chemical Durability Phosphate Glasses, Cobalt Oxide, Density, DTA, DRX,

IR, SEM Micrograph

1. Introduction

Due to their poor chemical durability phosphate glasses have rather limited technological application despite their investigation so far conducted by many researchers [1] [2]. However, several phosphate glasses with high aqueous corrosion resistance have been reported [3] [4] [5] [6] [7]. Their properties (low melting point, high thermal expansion coefficient, bioactivity, optical properties etc.) make these glasses serious potential candidates for many technological applications. It has been found that the introduction of oxides, such as ZnO, Fe₂O₃, Al₂O₃, PbO, CaO and Cr₂O₃, results in the formation of, Zn-O-P, Fe-O-P, Pb-O-P, Al-O-P, Ca-O-P and Cr-O-P bonds, leading to improvement of phosphate glasses chemical durability [5] [7] [8] [9] [10] [11]. The synergy of phosphate glasses with some types of nuclear waste has indicated the possibility of a form of waste with a lower corrosion rate than borosilicate glasses [8] [12]. As a result of high chemical durability, iron phosphate glasses have been considered as better candidates for the vitrifying of some type of nuclear wastes when compared with borosilicate glasses [4] [5] [6] [8]. The aim of the present work is to synthesize and select phosphate glasses in the system 50P₂O₅-25CaO-(25-x)Na₂O-xCoO (with 0 ≤ x ≤ 25; mol%) for two reasons:

- the first reason is to analyze glasses, with low cobalt content, by different techniques arranged for further later studies in the biomedical field [13] [14] [15];
- the second reason is to compare the effect of cobalt with that of iron in inhibition of corrosion [3] [6] [16]. The studied series indicated the structural change when cobalt content increases and causes an important tendency polymerization from orthophosphates to pyrophosphate groups which are at the origin of the improvement of chemical durability.

2. Experimental Section

Phosphate glasses are prepared by direct melting of the (NH₄)H₂PO₄ (98,99% pure), CaCO₃ (99.5% pure), Na₂O (99% pure), CoCO₃, xH₂O (Co 43% - 47% pure) mixtures with suitable proportions. The reagents are intimately crushed then introduced into a porcelain crucible. They were initially heated at 300 °C for 2 h and then kept at 500 °C for 1 h to complete the decomposition. The reaction mixture was then heated at 850 °C. for 1 h and finally at 1080 °C for 30 minutes. The homogeneous liquid was poured in aluminum plate previously heated to 200 °C to avoid thermal shock. Pellets about 5 to 10 mm in diameter and 1 to 3 mm thick were obtained. The samples were polished with carbon Silica sandpaper (with CSI of sufficiently high level), cleaned with acetone and immersed in pyrex beakers containing 100 ml of distilled water and carried to 90 °C. The sample surface must be constantly submerged in distilled water for 21 consecu-

tive days. The dissolution rate was evaluated from the mass loss as a function of time. The IR spectra of the studied phosphate glasses were determined in the frequency range between 400 and 1600 cm^{-1} with a resolution of 2 cm^{-1} using a Fourier transform infrared spectrometer (IR AFFINITY-1S). The samples were finally ground and mixed with KBr (potassium bromide), which is transparent in the IR and serves as a template. The ratio of the matter/KBr in the pellets was 10% by weight. The vitreous state was first evidenced from the shiny and transparency aspect, which was confirmed by X-ray diffraction patterns (XRD type BRUKER D8 ADVANCE). The glasses S_0 , S_2 and S_4 were annealed at 540 °C, 551 °C and 660 °C, respectively, for 72 hours. Differential thermal analysis (DTA) was performed using a DTG-60 SUMULTANEOUS DTA-DTG Apparatus, at a heating rate of 10 °C/min in atmospheric air with alumina crucibles. The Archimedes method was used to measure the density of glasses using orthophthalate as a floating medium. The microstructures of the sample glasses were characterized by scanning electron microscopy (SEM), equipped with a full system micro-analyser (EDX-EDAX).

3. Results and Discussion

3.1. Analysis of Chemical Durability of Series Glasses 50P₂O₅-25CaO-(25-x)Na₂O-xCoO

The chemical durability (D_R) of the glass series 50P₂O₅-25CaO-(25-x)Na₂O-xCoO (with $0 \leq x \leq 25$ mol%) was determined from the dissolution rate (D_R) of the samples immersed in 100 ml of distilled water at 90 °C for 21 consecutive days. The dissolution rate is defined as the weight loss of the glass expressed in $\text{g}\cdot\text{cm}^{-2}\cdot\text{min}^{-1}$. The values of D_R and of pH of the leaching aqueous solution are represented respectively, in figures 1 and grouped in Table 1. In Figure 1, the shape of the D_R curve indicates a progressive improvement of the chemical durability of the glass from 5.44×10^{-5} to 8.60×10^{-7} ($\text{g}\cdot\text{cm}^{-2}\cdot\text{min}^{-1}$) when the CoO content varies from 0 to 25 mol% [10].

3.2. Density and Molar Volumes

Density measurements allowed us to follow the evolution of the molar volume

Table 1. Compositions, calculated O/P ratio, D_R and transition temperature (T_g) of the series 50P₂O₅-25CaO-(25-x)Na₂O-xCoO glasses versus CoO (mol%).

Glass Sample	Starting glass composition (mol%)				Ratio O/P	D_R ($\text{g}/\text{cm}^2\cdot\text{min}$)	T_g (°C)	T_c (°C)	T_c-T_g	pH ± 0.5
	CoO	Na ₂ O	CaO	P ₂ O ₅			(±5 °C)			
S_0	0	25	25	50		$(5.40 \pm 0.20) \times 10^{-5}$	377	505	128	6,2
S_1	5	20	25	50		$(1.69 \pm 0.20) \times 10^{-5}$	405	524	119	6,6
S_2	10	15	25	50	3	$(4.83 \pm 0.20) \times 10^{-6}$	434	555	121	8,4
S_3	15	10	25	50		$(1.55 \pm 0.20) \times 10^{-6}$	455	570	115	8,6
S_4	25	0	25	50		$(8.60 \pm 0.20) \times 10^{-7}$	528	661	133	8,8

depending on the composition of the system $50\text{P}_2\text{O}_5\text{-}25\text{CaO}\text{-(}25\text{-x)}\text{Na}_2\text{O}\text{-xCoO}$. The density measurements were completed at room temperature. As can be observed from **Figure 2**, the variation in density versus CoO content (mol%) indicates an increase of density. On the other hand, it was possible to deduce the value of the molar volume and oxygen radius from density measurements, calculated from the approximate hypothesis of the close packing of oxygen anions, O^{2-} , each having $r_{\text{cal}}(\text{O}^{2-})$ recapitulated for each composition in **Table 2** [4] [10] [16] [17]. The molar volume of oxygen and the radius of anions of oxygen (O^{2-}) in the glass have been determined from Equations (1) and (2), respectively.

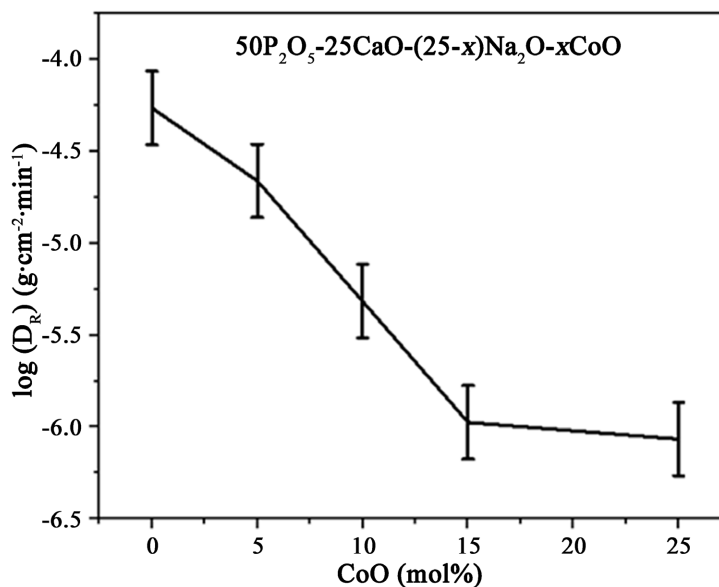


Figure 1. Dissolution rates (D_R) of the series of $50\text{P}_2\text{O}_5\text{-}25\text{CaO}\text{-(}25\text{-x)}\text{Na}_2\text{O}\text{-xCoO}$ glasses versus CoO (mol%).

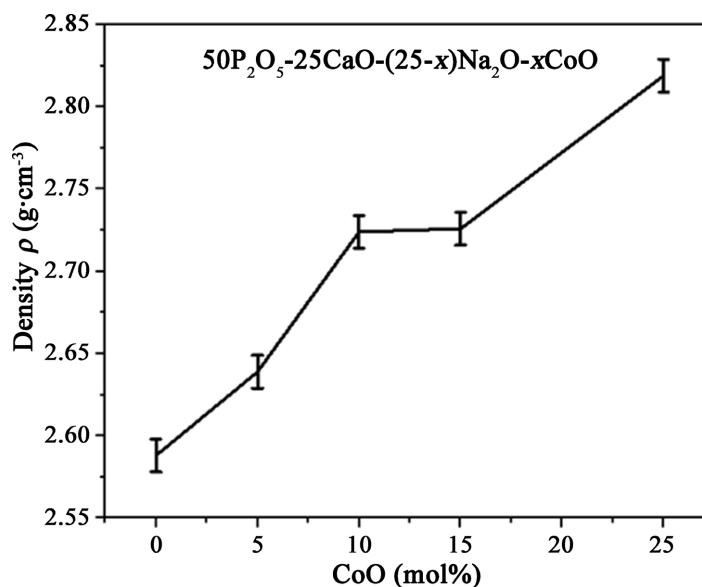


Figure 2. Variation of the density (ρ) versus CoO (mol%) along the glasses series $50\text{P}_2\text{O}_5\text{-}25\text{CaO}\text{-(}25\text{-x)}\text{Na}_2\text{O}\text{-xCoO}$.

Table 2. Density and related molar data of the 48P₂O₅-30CaO-(21-x)Na₂O-xTiO₂ system.

Samples	Molar formula Oxygène/Mol (N _o)	Density ρ_v (g·cm ⁻³)	Molar Mass (g/mol)	Molar Volume (Å) ³ $V_{OM} = \frac{M}{\rho N_A N_o}$	Calculated oxygen radius (O ²⁻) (Å) $r_{cal}(O^{-2})$
S ₀	25Na ₂ O-25CaO-50P ₂ O ₅ (300)	2.588	10,051.95	21.5	1.390
S ₁	5CoO-20Na ₂ O-25CaO-50P ₂ O ₅ (300)	2.637	10,116.615	21.2	1.384
S ₂	10CoO-15Na ₂ O-25CaO-50P ₂ O ₅ (300)	2.709	10,181.28	20.8	1.375
S ₃	15CoO-10Na ₂ O-25CaO-50P ₂ O ₅ (300)	2.720	10,245.945	20.6	1.372
S ₄	25CoO-25CaO-50P ₂ O ₅ (300)	2.819	10,375.275	20.3	1.364

$$V_{OM} = M / \rho N_A * N_o \quad (1)$$

$$r_{cal}(O^{-2}) = \frac{\sqrt[3]{V_{OM}}}{2} \quad (2)$$

With M = molar mass, ρ = density, N_A = Avogadro number; $*N_o$ = number of oxygen atoms in the molecular formula. A detailed analysis of the data in **Table 2** shows that the molar volume decreases increasing of the CoO content. The covalent radius value of the oxygen atom (O²⁻), calculated by the molar volume using the Equation (2) for each composition, decrease, also, indicating a reinforcement of the metal-oxygen-phosphorus (Co-O-P) bond with increasing of CoO content.

3.3. Structural Approach by Infrared Spectroscopy

Infrared spectra of glass series 50P₂O₅-25CaO-(25-x)Na₂O-xCoO (0 ≤ x ≤ 25; mol%) are shown in **Figure 3**. The assignments of the vibration bands are given in **Table 3**. All vibration bands of treated phosphate glasses are shown in the range of frequencies between 400 and 1600 cm⁻¹. The band at 490 - 510 cm⁻¹ is attributed to skeletal deformation δ_{ske} (P-O-P) [3] [4] [5] [6] [18]. The frequency band located at 770 - 786 cm⁻¹ is attributed to the symmetrical mode of vibration ν_{sym} (P-O-P) of the pyrophosphate groups (Q1) [4] [18] [19] [20] [21], while the bands at 880 - 910 are assigned to the asymmetric vibration mode ν_{asym} (P-O-P) [4] [8] [22] [23] [24] [25] [26]. The band that appears around 1015 cm⁻¹ is attributed to the asymmetric vibration mode ν_{asym} (P-O-P) of the isolated orthophosphate groups (Q^o) [5] [19] [21] [23]. The band at 1280 cm⁻¹ is attributed to asymmetric stretching of two non-bridging oxygens ν_{sym} PO₂. Analysis of the IR spectra obtained (**Figure 3**) indicates that the vibration band ν_{asym} P-O-P at 1015 cm⁻¹ attributed to the isolated orthophosphate groups decreases with increasing cobalt oxide at the expense of Na₂O content. This band disappears completely when the CoO content reaches 15 mol%. On the other hand the shift, at the

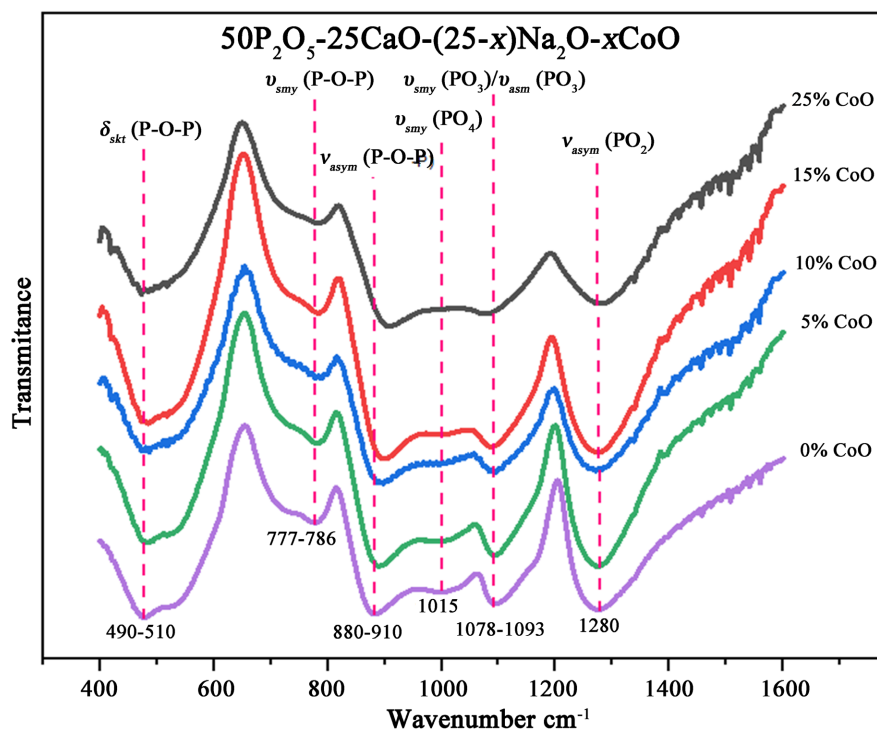


Figure 3. IR spectra of the series of $50\text{P}_2\text{O}_5\text{-}25\text{CaO}\text{-(}25\text{-}x\text{)Na}_2\text{O}\text{-}x\text{CoO}$ glasses, (with $0 \leq x \leq 25$; mol%).

Table 3. The assignments of different vibration bands of the IR spectra of the quaternary $50\text{P}_2\text{O}_5\text{-}25\text{CaO}\text{-(}25\text{-}x\text{)Na}_2\text{O}\text{-}x\text{CoO}$.

Régions de fréquence (cm ⁻¹)	assignements	Références
490 - 510	Vibration mode δ_{ske} (P-O-P)	[3] [4] [5] [6] [14] [19] [20] [21] [22] [23]
777 - 786	Vibration mode ν_{sym} (P-O-P) in unit Q ¹	[14] [18] [19] [20]
880 - 910	Vibration mode ν_{asym} (P-O-P) in unit Q ¹	[5] [18] [19]
1015	Vibration mode ν_{asym} (P-O-P) in unit Q ⁰	[5] [23] [27]
1078 - 1093	Vibration mode $\nu_{sym}(\text{PO}_2)/\nu_{asym}(\text{PO}_3)$ in units Q ¹ + Q ²	[20]
1280	Vibration mode $\nu_{asym}(\text{PO}_2)$ in unit Q ²	[3] [4] [5] [19] [26] [27]

same time, of the vibration band ν_{sym} P-O-P, located at 777 cm^{-1} , towards the high values and the decrease in the intensity of the vibration band ν_{PO_2} , located at 1280 cm^{-1} , added the shift of the vibration band $\nu_{asym}(\text{PO}_3)/\nu_{sym}(\text{PO}_2)$ toward low values, confirms the increase in the number of pyrophosphate groups to the detriment of metaphosphate groups, when the CoO content increases in the glass network. As for the vibration bands at approximately $1078\text{-}1093\text{ cm}^{-1}$ and 1280 cm^{-1} are assigned, respectively, to the stretching vibration mode $\nu_{asym}(\text{PO}_3)/\nu_{sym}(\text{PO}_2)$ attributed of the pyrophosphate groups and to the vibration mode $\nu_{asym}(\text{PO}_2)$ attributed to metaphosphate groups (Q²) [3] [4] [9] [20] [21] [26] [27]

3.4. X-Ray Diffraction and DTA Analysis

As expected, X-ray diffractions have confirmed the vitreous character of all of

the investigated glass samples (see **Figure 4**). DTA analysis of the phosphate glass $50\text{P}_2\text{O}_5\text{-}25\text{CaO}\text{-}(25\text{-}x)\text{Na}_2\text{O}\text{-}x\text{CoO}$ (with $0 \leq x \leq 25$; mol%), shown in **Figure 5**, indicates both an increase in the glass transition temperature and the crystallisation temperature versus the CoO content. When the CoO content increases from 0 to 25 mol%, the glass transition temperature (T_g) increases in the 399°C - 477°C range, whereas the crystallisation temperature (T_c) increases in the 502°C - 657°C range (**Table 1**). The $T_c\text{-}T_g$ difference is significant, which explains the high thermal stability [13] [28]. The heat treatments of the S_0 , S_2 and S_4 glasses at 540°C , 551°C and 660°C for 72 h, respectively, give the XRD patterns shown in **Figure 6**. These spectra show a structural evolution from orthophosphate ($\text{O/P} = 4$) and oligophosphate phases ($3 \leq \text{O/P} \leq 3.5$) to oligophosphate phase with majority of pyrophosphates phases (Q^1). When the S_0 sample was thermally treated at 540°C , the amorphous phase partially disappeared and major Ca_3PO_4 [JCPDS file N°: 00-009-0340], NaCaPO_4 [JCPDS file N°: 00-029-1193] and Na_3PO_4 [JCPDS file N°: 00-031] occurred in the sample, with minor NaPO_3 [JCPDS file N°: 00-002-0776], $\text{Ca}(\text{PO}_3)_2$ [JCPDS file N°: 00-017-0500], CaP_2O_6 [JCPDS file N°: 00-015-0204], and $\text{Ca}_2\text{P}_2\text{O}_7$ [JCPDS file N°: 00-009-0346] phases. When the CaO content increased in the S_2 glass, the heat treatment at 551°C

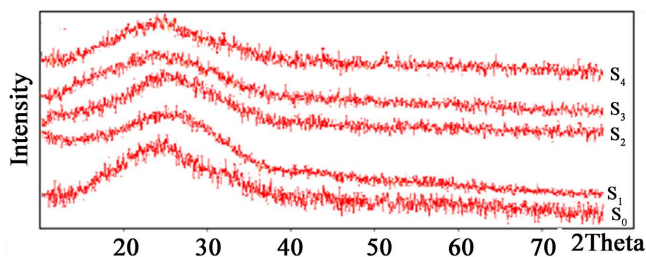


Figure 4. XRD patterns for glass samples S_0 , S_1 , S_2 , S_3 and S_4 .

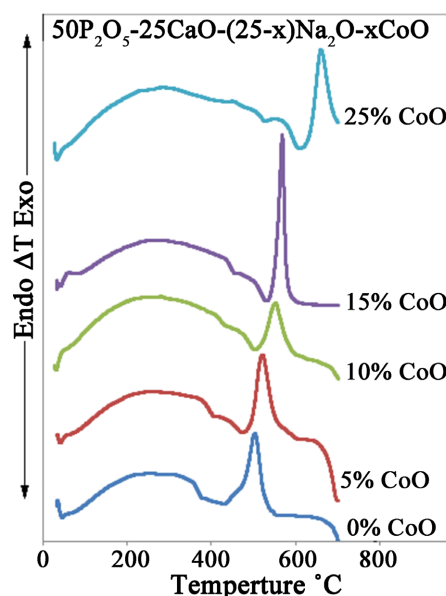


Figure 5. Differential thermal analysis (DTA) of the series of $50\text{P}_2\text{O}_5\text{-}25\text{CaO}\text{-}(25\text{-}x)\text{Na}_2\text{O}\text{-}x\text{CoO}$ CoO glasses versus CoO (mol%).

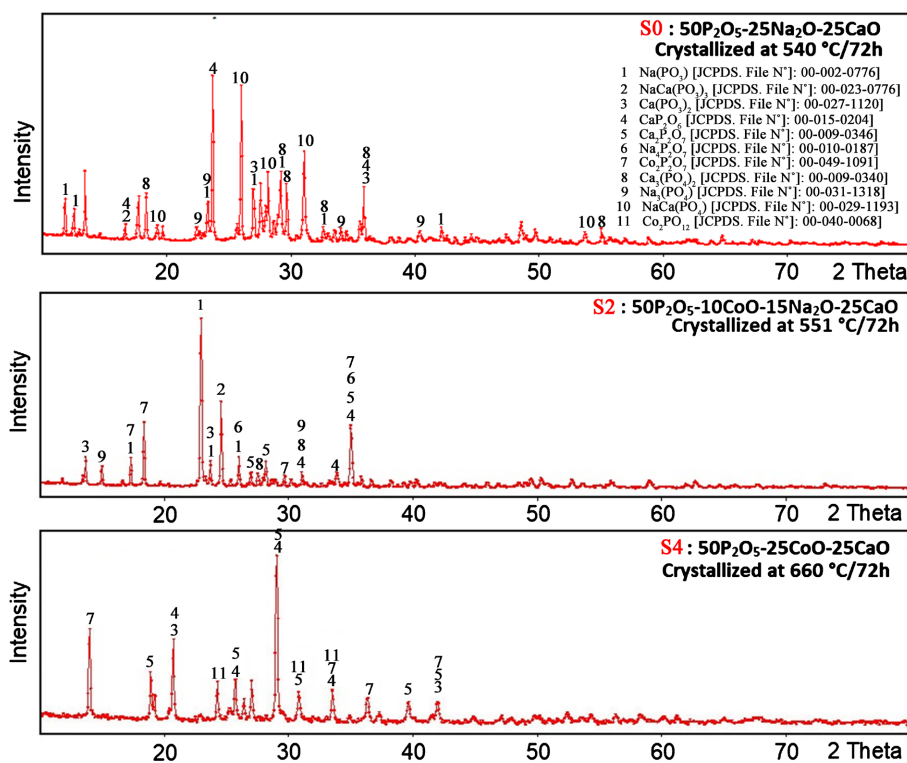


Figure 6. X-ray diffraction spectra, after heat treatment at crystallization temperatures 508 °C, 560 °C and 680 °C for 72 h, respectively, for S₀, S₂ and S₄.

caused the formation of Na₂P₂O₇, [JCPDS file N°: -], Ca₂P₂O₇ [JCPDS file N°: 00-009-0346] and Co₂P₂O₇ [JCPDS file N°: 00-040-0068] with some traces of metaphosphate and isolated short orthophosphates phases. However, when the CoO content increased to 25 mol%, the heat treatment, at 660 °C, indicated the disappearance of the isolated ortho-phosphate phases, while the CaP₂O₆ phases [JCPDS file N°: 01-015-0204], Ca(PO₃)₂ [JCPDS file N°: 00-009-0363], Co₂P₄O₁₂ [JCPDS file N°: 00-040-0068], Co(PO₃)₂, [JCPDS file N°: 00-027-1120], Ca₂P₂O₇ [JCPDS file N°: 00-009-0346], and Co₂P₂O₇ [JCPDS file N°: 00-040-0068] appeared largely in the sample with very high intensities that confirms the results obtained by IR [13].

3.5. SEM Micrograph Analysis

SEM images in **Figure 7** illustrate the morphology of the glasses considered in this work. The glass form of S₁ shown in **Figure 7(a)**, exhibit the presence crystalline phases with different form and size [5] [9] [10] [23]. When the CoO content increases in the glass, the number of crystallites decreases. Hence, SEM analysis confirms a homogenous vitreous phase with feeble crystalline particles in the S₄ sample (**Figure 7(e)**) which has the maximum CoO content. Some different crystalline phases were identified by XRD and it seems that a decrease of crystallisation tendency is enhanced and Co(PO₃)₂, Ca₂P₂O₇ and Co₂P₂O₇ phases are crystallized in the last sample (S₄) [13]. This probably explains the structural change towards more short pyrophosphates at the detriment of shorter isolated

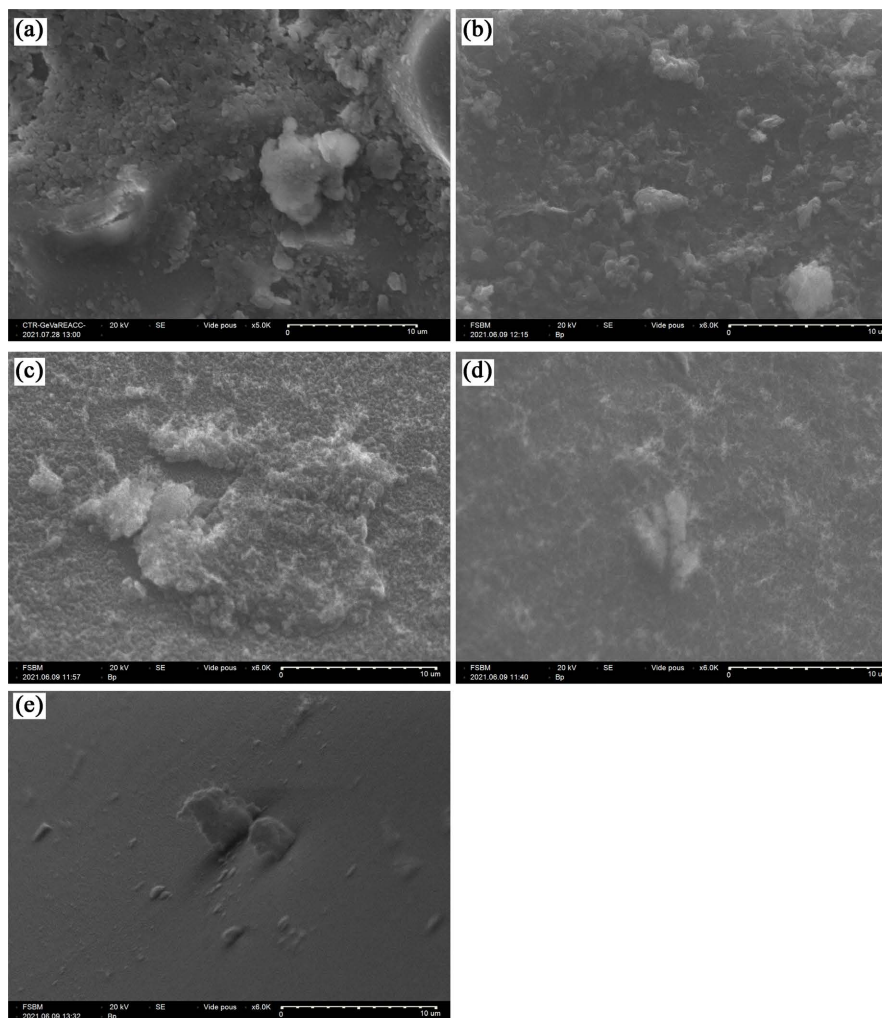


Figure 7. SEM micrographs (a)-(e), showing the structural evolution of phosphate glasses respectively from S_0 to S_4 .

orthophosphate chains as the CoO content increases in the glass network.

4. Discussion

The glasses series $50P_2O_5-25CaO-(25-x)Na_2O-xCoO$ (with $0 \leq x \leq 25$; mol%), were prepared by direct melting at $1080^\circ C$. The structure and the chemical durability of these glasses have been investigated using various techniques such as density, X-Ray, DTA, diffraction, IR and SEM. The study of the dissolution rate for all the glasses studied indicates an improvement in chemical durability when the CoO content increases to the detriment of Na_2O . The variation of transition temperature versus CoO content indicates an increase in T_g from $399^\circ C$ to $477^\circ C$ when the CoO content increases from 0. To 25 mol%, elucidating an improvement in the rigidity of the glass [8] [13] [18] [21] [28].

The specific mass (Density) of vitrified phosphates is increasing with molar fraction along the series. The covalent radius values of oxygen calculated from Equation (2) indicate that the minimum value $r_{cal}(O^{2-})$ is observed for $x = 20$

mol% and therefore a relatively high reinforcement of the metal-oxygen-phosphorus (Co-O-P) bond [4] [12] [17] [28]. On the other hand, Analysis of infrared spectra indicates that the increase of CoO content to the detriment of Na₂O, in phosphate glass, leads to the formation of oligophosphate groups (Q¹-Q²) [22] [28] with the majority pyrophosphates at the expense of orthophosphates and metaphosphates and or cyclical metaphosphates groups. X-ray diffraction analysis of glasses, annealed between 502°C to 663°C for 72 hours, confirms the evolution, with the increase of CoO content, of crystalline phases towards oligophosphate phase's rich of pyrophosphates. In fact, when the CoO content exceeds 15 mol%, the orthophosphate phases completely disappear in the vitreous network. Analysis of SEM micrograph indicates the evolution of the structural morphology of the glasses. As the CoO content increases in the glass, the number of crystallites decreases, consequently, SEM micrograph expected in **Figure 7(e)** for S₄ sample, having a maximum CoO content, confirms a homogeneous glass phase with low crystalline particles.

This phenomenon is explained by the fact that Na₂O (Na⁺ alkali ion) is a main modifier oxide which easily depolymerizes the vitreous network by creating increasingly short chains going from ultraphosphate chains to metaphosphate, pyrophosphate and shorter isolated orthophosphate chains [3] [5] [29]. This accentuated depolymerization leads to the formation of a large number of easily hydrated Na-O-P bonds which greatly reduce the chemical durability of the glasses. In addition, the effect of the oxide CaO which depolymerizes the glass from ultra-phosphate towards chains mainly of metaphosphate or cyclic metaphosphate, it can be explained that the increases of CoO to the detriment of Na₂O has the effect of polymerizing the structure from isolated orthophosphate chains toward the formation of oligophosphates predominately by pyrophosphate chains. This behavior leads to the replacement of hydrated Na-O-P, P-O-P and possibly Ca-O-P bands, by the covalent and resistant Co-O-P bonds.

Hence, the glasses series studies in the present work can be divided into three categories:

- 1) Glasses with a low CoO content (0.5 to 3 mol%) can be applied with a slight improvement in the optical field [19] [30] [31].
- 2) Glasses with CoO content between 5 and 15 mol% can be tested successfully in the biomedical field because they can increase the rigidity of the glass and participate in the osteoinduction of bone tissue [14] [15] [18] [31].
- 3) Glasses with content between 20 and 25 mole%, can be used, with some improvement, in the electrical conduction range since cobalt can be found under two degrees of oxidation Co²⁺ and Co³⁺ which ensures the hopping mechanism of the electrons and therefore oxidation reduction phenomenon [21] [32].

Hence, a better understanding of phosphate glass structure is very relevant to the industry in the development of technical glasses to achieve good performances.

5. Conclusions

The structure and properties of $x\text{CoO}-(25-x)\text{Na}_2\text{O}-25\text{CaO}-50\text{P}_2\text{O}_5$ phosphate glasses (with $0 \leq x \leq 25$; mol%) have been investigated in the present paper. Here are some conclusions from this paper:

- 1) The structure of the Co-Na-Ca-phosphate samples glasses, predominantly, consists of oligophosphate, Q^2 - Q^1 units, and the CoO leads to the conversion of Q^0 units to Q^1 units.
- 2) The glass transition temperature is improved by increasing CoO content in the glass network and leads to the increase of thermal stability.
- 3) Increasing the glass transition temperature leads to improved chemical durability.
- 4) The SEM Micrograph indicates an obvious decrease in crystallites with the increase in CoO, causing a relatively large equilibrium between the glass bath and the crystallites.

Acknowledgements

The authors would like to thank the technical analysis and characterization center of Faculty of Sciences, Ain chock, Casablanca, for the help in the realization of this work.

Conflicts of Interest

The authors declare no conflicts of interest regarding the publication of this paper.

References

- [1] Bunker, B.C., Arnold, G.W. and Ao Wilder, J. (1984) Phosphate Glass Dissolution in Aqueous Solutions. *Journal of Non-Crystalline Solids*, **64**, 291-316. [https://doi.org/10.1016/0022-3093\(84\)90184-4](https://doi.org/10.1016/0022-3093(84)90184-4)
- [2] Gao, H.S., Tan, T. and Wang, D.H. (2004) Dissolution Mechanism and Release Kinetics of Phosphate Controlled Release Glasses in Aqueous Medium. *Journal of Controlled Release*, **96**, 29-36. <https://doi.org/10.1016/j.jconrel.2003.12.031>
- [3] Aqdim, S., *et al.* (2012) Chemical Durability and Structural Approach of the Glass Series $(40-y)\text{Na}_2\text{O}-y\text{Fe}_2\text{O}_3-5\text{Al}_2\text{O}_3-55\text{P}_2\text{O}_5$ -by IR, X-Ray Diffraction and Mössbauer Spectroscopy. *IOP Conference Series: Materials Science and Engineering*, **27**, Article ID: 012003. <https://doi.org/10.1088/1757-899X/28/1/012003>
- [4] Aqdim, S., El Hassan, S. and Brahim, E. (2008) Structural and Durability Investigation of the Vitreous Part of the System $(35-z)\text{Na}_2\text{O}-z\text{Fe}_2\text{O}_3-5\text{Al}_2\text{O}_3-60\text{P}_2\text{O}_5$. *Eurasian Chemico-Technological Journal*, **10**, 9-17.
- [5] Beloued, N., Chabbou, Z. and Aqdim, S. (2016) Correlation between Chemical Durability Behaviour and Structural Approach of the Vitreous Part of the System $55\text{P}_2\text{O}_5-2\text{Cr}_2\text{O}_3-(43-x)\text{Na}_2\text{O}-x\text{PbO}$. *Advances in Materials Physics and Chemistry*, **6**, 149-156. <https://doi.org/10.4236/ampc.2016.66016>
- [6] Makhkhas, Y., Said, A. and El Hassan, S. (2013) Study of Sodium-Chromium-Iron-Phosphate Glass by XRD, IR, Chemical Durability and SEM. *Journal of Materials Science and Chemical Engineering*, **1**, 1-6.

- <https://doi.org/10.4236/msce.2013.13001>
- [7] Ahmed, I., *et al.* (2004) Phosphate Glasses for Tissue Engineering: Part 2. Processing and Characterisation of a Ternary-Based P_2O_5 -CaO-Na₂O Glass Fibre System. *Biomaterials*, **25**, 501-507. [https://doi.org/10.1016/S0142-9612\(03\)00547-7](https://doi.org/10.1016/S0142-9612(03)00547-7)
- [8] Sales, B.C. and Boatner, L.A. (1984) Lead-Iron Phosphate Glass: A Stable Storage Medium for High-Level Nuclear Waste. *Science*, **226**, 45-48. <https://doi.org/10.1126/science.226.4670.45>
- [9] Aqdim, S. (2013) Elaboration and Structural Investigation of Iron (III) Phosphate Glasses. *Advances in Materials Physics and Chemistry*, **3**, 332. <https://doi.org/10.4236/ampc.2013.38046>
- [10] Chabbou, Z. and Said, A. (2014) Chemical Durability and Structural Proprieties of the Vitreous Part of the System $xCaO$ -(40-x)ZnO-15Na₂O-45P₂O₅. *Advances in Materials Physics and Chemistry*, **4**, 179. <https://doi.org/10.4236/ampc.2014.410021>
- [11] Abou Neel, E.A., *et al.* (2015) Characterisation of Antibacterial Copper Releasing Degradable Phosphate Glass Fibres. *Biomaterials*, **26**, 2247-2254. <https://doi.org/10.1016/j.biomaterials.2004.07.024>
- [12] Huang, W.H., *et al.* (2004) Vitrification of High Chrome Oxide Nuclear Waste in Iron Phosphate Glasses. *Journal of Nuclear Materials*, **327**, 46-57. <https://doi.org/10.1016/j.jnucmat.2004.01.021>
- [13] Er-Rouissi, Y., *et al.* (2020) Chemical Durability, Structure Properties and Bioactivity of Glasses $48P_2O_5$ -30CaO-(22-x)Na₂O-xTiO₂ (with $0 < x \leq 3$; mol%). *Advances in Materials Physics and Chemistry*, **10**, 305-318. <https://doi.org/10.4236/ampc.2020.1012024>
- [14] Sobhanachalama, P., Ravi Kumar, V., Raghavaiah, B.V., *et al.* (2017) *In Vitro* Investigations on CoO Doped CaF₂-CaO-B₂O₃-P₂O₅-MO Bioactive Glasses by Means of Spectroscopic Studies. *Optical Materials*, **73**, 623-637. <https://doi.org/10.1016/j.optmat.2017.09.022>
- [15] Vyas, V.K., *et al.* (2016) Effect of Cobalt Oxide Substitution on Mechanical Behaviour and Elastic Properties of Bioactive Glass and Glass-Ceramics. *Transactions of the Indian Ceramic Society*, **75**, 12-19.
- [16] Beloued, N., *et al.* (2019) Relationship between Chemical Durability, Structure and the Ionic-Covalent Character of Me-OP Bond (Me = Cr, Fe), in the Vitreous Part of the System $60P_2O_5$ -2Cr₂O₃-(38-x)Na₂O-xFe₂O₃ (with $3 \leq x \leq 33$ mol%). *Advances in Materials Physics and Chemistry*, **9**, 199.
- [17] Makhlouk, R., Beloued, N. and Aqdim, S. (2018) Study of Chromium-Lead-Phosphate Glasses by XRD, IR, Density and Chemical Durability. *Advances in Materials Physics and Chemistry*, **8**, 269-280. <https://doi.org/10.4236/ampc.2018.86018>
- [18] Lee, I.-H., *et al.* (2013) Development, Characterisation and Biocompatibility Testing of a Cobalt-Containing Titanium Phosphate-Based Glass for Engineering of Vascularized Hard Tissues. *Materials Science and Engineering: C*, **33**, 2104-2112. <https://doi.org/10.1016/j.msec.2013.01.024>
- [19] Abdelghany, A.M., *et al.* (2018) Optical and FTIR Structural Studies on CoO-Doped Strontium Phosphate Glasses. *Journal of Non-Crystalline Solids*, **499**, 153-158. <https://doi.org/10.1016/j.jnoncrysol.2018.07.022>
- [20] Liu, H.S., Chin, T.S. and Yung, S.W. (1997) FTIR and XPS Studies of Low-Melting PbO-ZnO-P₂O₅ Glasses. *Materials Chemistry and Physics*, **50**, 1-10. [https://doi.org/10.1016/S0254-0584\(97\)80175-7](https://doi.org/10.1016/S0254-0584(97)80175-7)
- [21] Jerroudi, M., *et al.* (2021) Structure-Property Correlations in Lithium Zinc Cobalt Metaphosphate Glasses and Glass-Ceramic. *Physica B: Physics of Condensed Matter*

- Physica B*, **610**, Article ID: 412949. <https://doi.org/10.1016/j.physb.2021.412949>
- [22] Vast, P. and Semmoud, A. (1994) Comportement thermique du difluorodioxophosphate ferreux. *Journal of Thermal Analysis and Calorimetry*, **41**, 1489-1493. <https://doi.org/10.1007/BF02549945>
- [23] Navarro, M., et al. (2008) Surface Characterization and Cell Response of a PLA/CaP Glass Biodegradable Composite Material. *Journal of Biomedical Materials Research Part A: An Official Journal of the Society for Biomaterials, the Japanese Society for Biomaterials, and the Australian Society for Biomaterials and the Korean Society for Biomaterials*, **85**, 477-486. <https://doi.org/10.1002/jbm.a.31546>
- [24] Šantić, A., et al. (2007) Structural Properties of Cr₂O₃-Fe₂O₃-P₂O₅ Glasses, Part I. *Journal of non-Crystalline Solids*, **353**, 1070-1077. <https://doi.org/10.1016/j.jnoncrysol.2006.12.104>
- [25] Reis, S.T., et al. (2002) Structural Features of Lead Iron Phosphate Glasses. *Journal of Non-Crystalline Solids*, **304**, 188-194. [https://doi.org/10.1016/S0022-3093\(02\)01021-9](https://doi.org/10.1016/S0022-3093(02)01021-9)
- [26] Brow, R.K., et al. (1995) The Short-Range Structure of Zinc Polyphosphate Glass. *Journal of Non-Crystalline Solids*, **191**, 45-55. [https://doi.org/10.1016/0022-3093\(95\)00289-8](https://doi.org/10.1016/0022-3093(95)00289-8)
- [27] Hudgens, J.J. and Martin, S.W. (1993) Glass Transition and Infrared Spectra of Low-Alkali, Anhydrous Lithium Phosphate Glasses. *Journal of the American Ceramic Society*, **76**, 1691-1696. <https://doi.org/10.1111/j.1151-2916.1993.tb06636.x>
- [28] Aqdim, S., Albizane, A. and Greneche, J.M. (2015) Structural Feature and Chemical Durability of Sodium Aluminium Iron Phosphate Glasses. *Journal of Environmental Science, Computer Science and Engineering & Technology*, **4**, 509-521.
- [29] Aqdim, S., et al. (2017) Elaboration and Characterization of Glasses and Ceramic-Glasses within the Ternary Diagram Li₂O-Cr₂O₃-P₂O₅. *Advances in Materials Physics and Chemistry*, **7**, 123-137. <https://doi.org/10.4236/ampc.2017.74011>
- [30] Abu-Khadra, A.S., et al. (2021) Effect of Silver Iodide (AgI) on Structural and Optical Properties of Cobalt Doped Lead-Borate Glasses. *Ceramic International*, **47**, 26271-26279. <https://doi.org/10.1016/j.ceramint.2021.06.036>
- [31] Ibrahim, A. and Sadeq, M.S. (2021) Influence of Cobalt Oxide on the Structure, Optical Transitions and Ligand Field Parameters of Lithium Phosphate Glasses. *Ceramic International*, **47**, 28536-28542. <https://doi.org/10.1016/j.ceramint.2021.07.011>
- [32] Choudhary, B.P. and Singh, N.B. (2016) Properties of Silver Phosphate Glass in the Presence of Nanosize Cobalt and Nickel Oxides. *Journal of Non-Crystalline Solids*, **440**, 59-69. <https://doi.org/10.1016/j.jnoncrysol.2016.02.015>